Asian Herpetological Research 2012, 3(1): 69–78
DOI: 10.3724/SP.J.1245.2012.00069

Ultrastructural Study of Limb Bud Development in Green Turtles *Chelonia mydas*

Nawal AL-MUKHAINI[1], Taher BA-OMAR[2*] and Ibrahim MAHMOUD[2]

[1] *Human and Clinical Anatomy Department*, *College of Medicine and Health Sciences*, *Sultan Qaboos University*, *P. O. Box* 35, *Muscat* 123, *Oman*
[2] *Biology Department*, *College of Science*, *Sultan Qaboos University*, *P. O. Box* 36, *Muscat* 123, *Oman*

Abstract Morphological changes during the embryonic development of limbs of the green turtle, *Chelonia mydas*, were studied during the entire period of incubation, using transmission and scanning electron microscopy (TEM and SEM). Limb buds were first observed at Stage 2. At that stage, the tip was covered with an apical ectodermal ridge (AER) which began to regress at Stage 6. Associated with AER was the presence of the mesenchymal cells which, consequently, differentiated into muscles, cartilage and bones. The gross features of the skeletal development appeared as a condensation of the cartilaginous structures in the proximal distal region of the limbs. The primordial digits were gradually enclosed by hard keratinized webbed skin. The increase in rate of ossification and skin pigmentation was correlated with the growth of the limbs. The development of the limbs was closely related to the transitional appearance of mucus secretion from the epidermis.

Keywords green turtle, *Chelonia mydas*, turtle embryology, limb bud development, ultrastructure

1. Introduction

The green turtle *Chelonia mydas* is among the most widely distributed species in tropical and temperate waters of the world (Sakai *et al.,* 2000). Ras Alhad Reserve, Oman has one of the largest nesting areas for green turtles in the Indian Ocean (Salm, 1991).

The developing limb bud in vertebrates consists of an ectodermal jacket filled with mesenchymal cells. During development, the mesenchymal cells differentiate into several cell types, amongst them are cartilage and muscle cells or may undergo programmed cell death. Cell differentiation is coordinated so that particular structures develop in a predictable temporo-spatial pattern, leading to an intricate pattern of vertebrate limb formation (Eichele, 1990).

The outgrowth of the limb bud in vertebrates is due to the changes in interaction between the mesoderm and the ectoderm (Borkhvardt, 2001). Zeller *et al* (2009) in their review article, stated that there is an integrative model during the morphogenic process of chicken and mice where all axes interact to proximal to distal outgrowth for patterning the process of limb bud formation.

In vertebrates, including chelonians, the formation of cartilage primordia of limb skeletal elements appears first, followed by the ossification process to establish the bony elements (Sheil, 2005). Some species of sea turtles show similarity in chondrification and ossification processes of the fore and hind limb elements, while others exhibit variations, especially in the patterns of ossification of the metapodial and phalangeal elements (Sheil, 2003; Sheil and Greenbaum, 2005; Sánchez-Villagra *et al.,* 2007).

Although some aspects of their biology are understood, ultrastructural studies of organs and appendages during development are scarce. Hence, this study was aimed to describe the ultrastructural characteristics of cellular changes in the developing limb buds of the green turtles using electron microscopy (TEM and SEM).

2. Material and Methods

Eggs from green turtles were collected randomly from

---

[*] Corresponding author: Dr. Taher BA-OMAR, from the College of Science, Sultan Qaboos University, Oman, with his research focusing on histological studies of different organs of *Aphanius dispar* (a Cyprinodant fish) and *Chelonia mydas*.
E-mail: taher@squ.edu.om

Received: 15 July 2011 Accepted: 10 Feburary 2012

13 nests for a total of 126 eggs within an area of 1 km^2 in Ras Alhad Reserve, Oman (22º 32' N, 59º 45' E to 22º 14' N, 59º 48' E). Each nest was excavated immediately after egg-laying and the eggs were transferred to plastic buckets containing wet sand within 12 h after oviposition. The eggs were then placed in SANYO incubators [free from Chloro Fluoro Carbons (CFC)] in the Department of Biology, Sultan Qaboos University (SQU), Oman. Incubation was adjusted to a constant temperature at 30ºC (± 0.05ºC). Each egg was incubated singly in a 600 ml plastic container according to the method of Mrosovsky (1988), with minor modifications. Each container had a plastic cover of 10 cm in diameter. The upper part of each container had six holes (2.5 mm in diameter) to provide ventilation and water exchange during incubation. Each egg was placed in the center of the container on top of spongy foam and then covered with vermiculite. Distilled water (65 ml) was added to each vermiculite container on d 0 and d 19 of incubation to ensure adequate humidity for development. An open 1-liter container with distilled water was placed at the bottom of the incubator to provide humidity for the eggs during incubation (Mrosovsky, 1988). Eggs were opened at 2–3 d intervals until hatching. For scanning electron microscopy (SEM), limb buds were dissected out after 7 d to 48 d of incubation, including pipping and hatchlings stages, and fixed in 4% Karnovsky' fixative buffered with sodium cacodylate adjusted to a pH of 7.4 for 4 h. Some limbs were dissected to show the internal structures at various stages. Afterwards, they were processed in a series of acetone and were then dried in a critical point dryer and sputter coated with gold. They were examined under a JEOL JEM-5600LV SEM.

For transmission electron microscopy (TEM), limb buds were dissected out after 14 d to 28 d of incubation and fixed in 4% Karnovsky's fixative buffered with sodium cacodylate adjusted to a pH of 7.4 for 4 h and then post-fixed in 1% aqueous solution of osmium tetroxide for 1 h. The limbs were dehydrated in a series of alcohol before embedding in Agar 100 resin. Semi-thin and ultra-thin sections were cut. The semi-thin sections were stained with toluidine blue and ultra-thin sections with super saturated uranyl acetate and lead citrate. The ultra-thin sections were examined under a JEOL JEM-1230 TEM.

A permit No.17/2008 for collecting turtle materials for scientific purposes was obtained from the Ministry of Environment and Climate Affairs, Sultanate of Oman. The specimens were deposited in the Biology Department Laboratory, SQU, Oman. The staging system of Al-Mukhaini *et al*. (2010) was used as a reference for identification patterns in the developing green turtles.

3. Results

The appearance of the fore- and hind limbs was first recorded on d 7 of incubation. Both limbs had similar patterns of development and most of the observations were based on the development of the forelimbs.

3.1 Scanning electron microscopy At Stage 3 (Figure 1), the forelimb bud extends approximately 4 somites in length, whereas the hindlimb bud extends approximately 3 somites. The apical ectodermal ridge (AER) is present. The cells covering the AER are packed tightly, while the cells covering the rest of the limb buds are dome shaped, loose and circular or cuboidal. Mucus pores are present over the entire outer cell surface with their mucus secretion.

At Stage 4 (Figure 2), pores with mucus are seen on the outer surface of the skin. The AERs were measured about 25 μm high. There is an elevation in the middle of the dorsal side of the paddle-shape forelimb bud. The squamous cells have various extensions and pores.

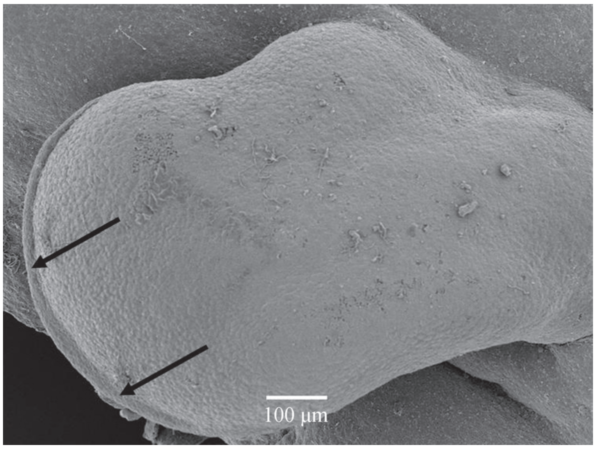

Figure 1 Electron micrograph of Stage 3 turtle embryo forelimb showing the apical ectodermal ridge (arrows). Scale bar = 100 μm.

At Stage 5 (Figure 3 A), the AER is thicker than that at the previous stages. There are extensive mucus secretions on the outer ectodermal skin covering the whole embryo.

At Stage 6 (Figure 3 B, C), the AER in both fore and hind-limbs begins to regress. There are two elevations on the middle part of the dorsal surface of forelimb. The distal ends of the limb exhibit folds between developing digits.

At Stage 9 (Figure 4 A), the claws appear in the forelimb protruding out of their sockets. Scales appear on the ventral and dorsal surfaces in a non-uniform pattern. The outer epidermal flat cells have a rough texture.

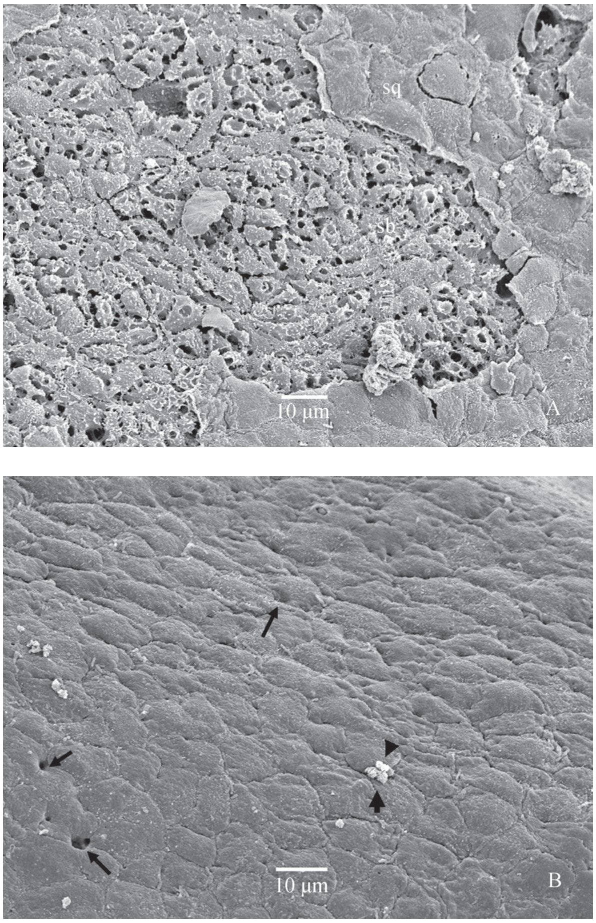

Figure 2 Electron micrographs of Stage 4 turtle embryo limb. A: Ectodermal cells with mucus droplets (arrow heads), mucous pores (arrows); B: Epidermal cells with squamous cells (sq) and the underlying mesenchymal cells (sb). Scale bar for both (A) and (B) = 10 µm.

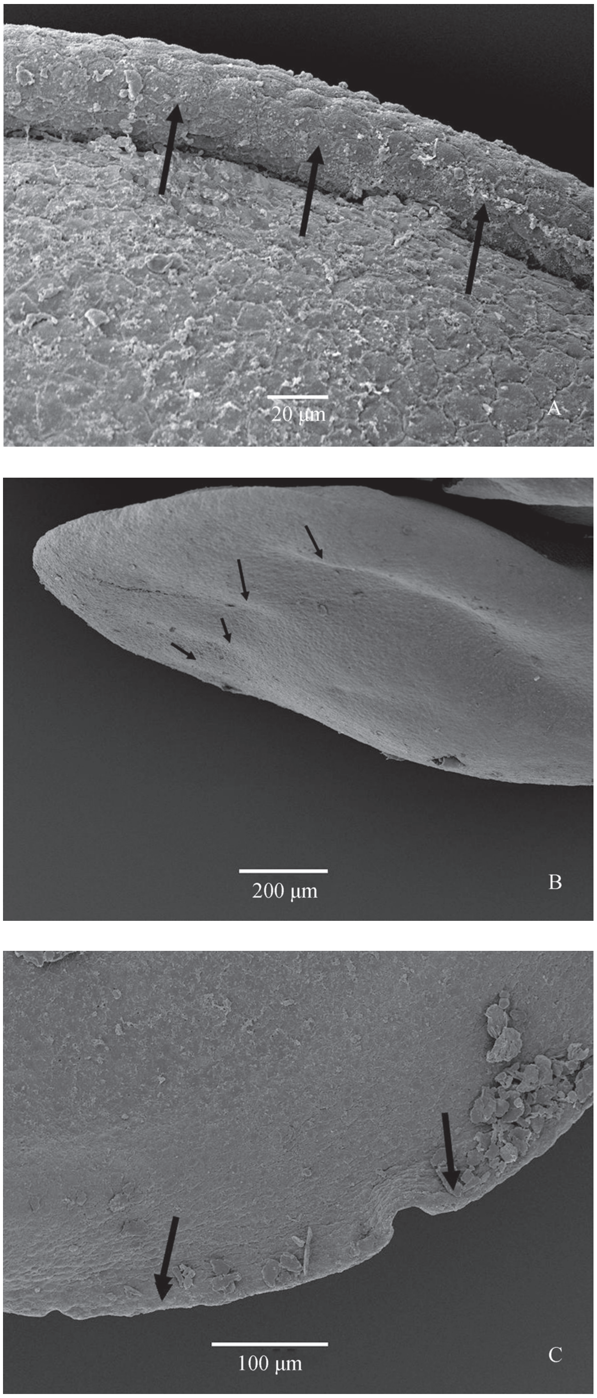

Figure 3 Electron micrographs of turtle embryo at Stage 5 (A), and Stage 6 (B and C). A: Apical ectodermal ridge (arrows); B: Four folds on the dorsal surface of the hindlimb (arrows); C: Regression of the apical ectodermal ridge (arrows). Scale bar: A = 20 µm, B = 200 µm and C = 100 µm.

At Stage 10 (Figure 4 B), the digital plate appears having five digits with their phalanges and interphalangeal joints. The digits are enclosed and connected by the webbed tissue forming a flipper. The distal margin of the flipper presents a folding with a wavy appearance. The middle digits are longer than those at the extreme sides of the flipper. The claw is rounded or blunt and its surface is covered by compact epidermal cells with pores and mucus drops. The epidermal outer covering cells show polygonal to hexagonal boundaries and have an extensive whitish sheet of microridges spreading across the surface.

At Stage 11 (Figure 5), the outer cellular layer of epidermis exhibits dense mucus and microridges texture with well-arranged polygonal cellular boundaries.

At Stage 12 (Figure 6), a cross section of the digit shows a cartilage core with chondrocytes, covered by the perichondrium. Skeletal muscle fibers are arranged in bundles. The layers beneath the skin layers are fibrous connective tissue with extensive collagen fibers and numerous blood vessels.

At Stage 13 (Figure 7), the outer epidermal layer exhibits compact polygonal cells. Some pores possess mucus droplet secretions (arrow in Figure 7A). The

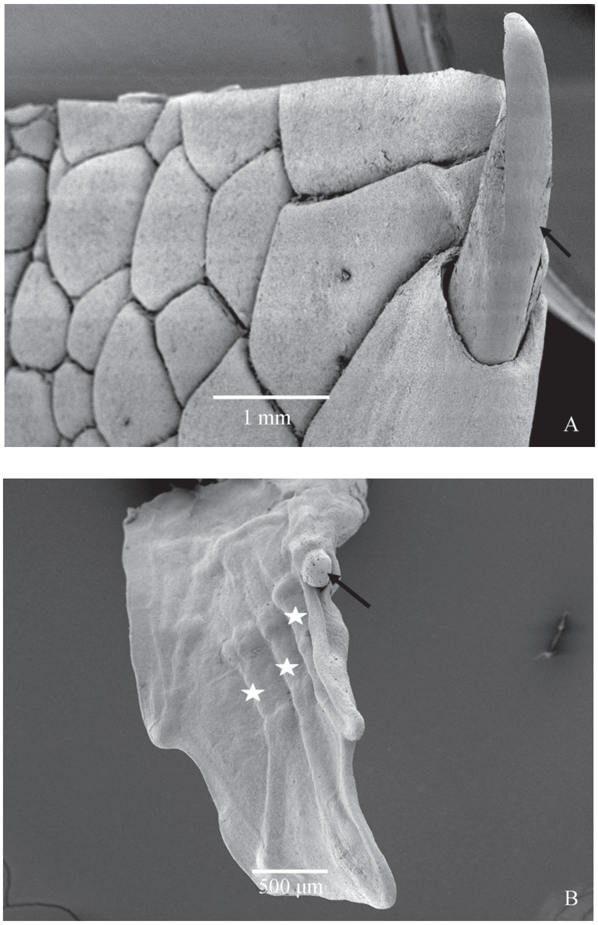

Figure 4 Electron micrographs of turtle embryo at Stage 9 (A) and Stage 10 (B). A: Ventral surface of the forelimb with a claw (arrow); B: An increase number of scales showing digital plates of the digits (stars) and one prominent claw (arrow). Scale bar: A = 1 mm and B = 500 μm.

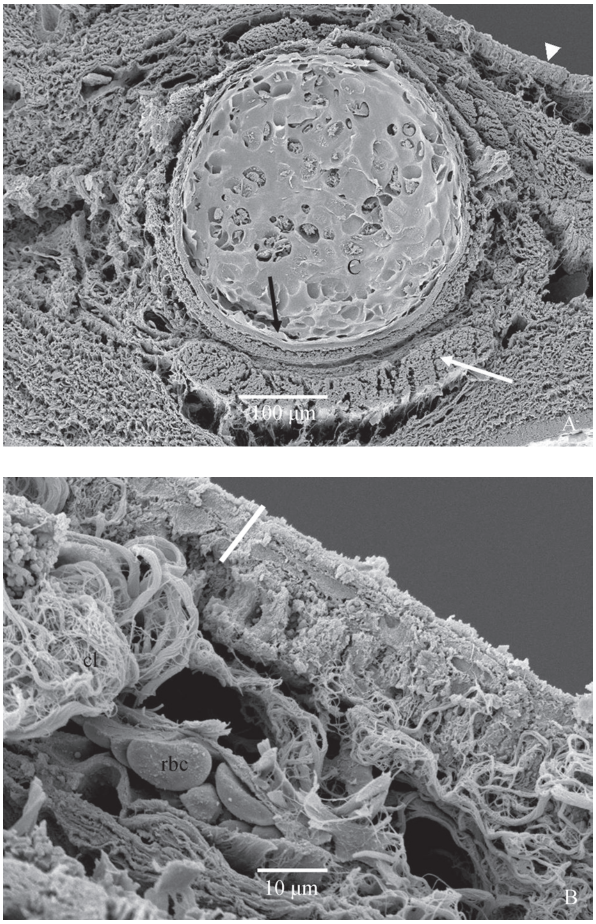

Figure 6 Electron micrographs of Stage 12 turtle embryo. A: Cartilage core (c) surrounded by perichondrium (black arrow), skeletal muscle bundles (white arrow) and epidermis (arrow head); B: Epidermis (white line), connective tissue, mainly collagenous fibers (cl) and blood vessels with red blood cells (rbc). Scale bar: A = 100 μm and B = 10 μm.

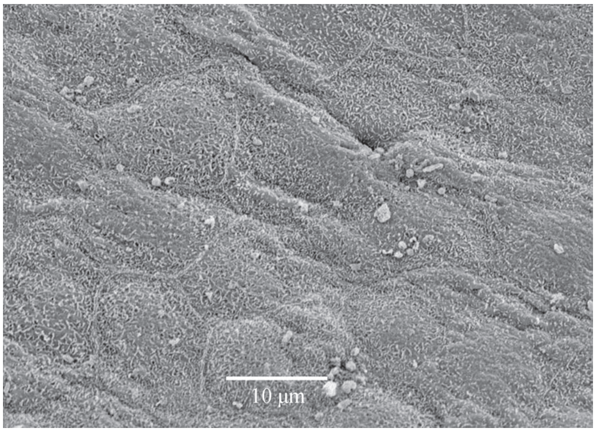

Figure 5 Electron micrograph of turtle embryo at Stage 11 showing outer epidermal cells. Scale bar = 10 μm.

epidermal layers are compact, and underlined by wavy dermis strata with abundance of collagenous fibers. The skeletal muscle bundles attach to the layers covering the cartilage core of the digit. The claws of the limbs are quite sharp and more bent than in the prior stage and exhibit epidermal cellular boundaries. The interdigital areas are mainly composed of connective tissue with collagenous fibers and blood vessels.

At Stage 14 (Figure 8), the outer covering of the skin exhibits many cellular wavy layers and the outermost layer shows well arranged cellular boundaries. Some digits, especially those in the middle, start to ossify by undergoing the process of endochondoral ossification.

At Stage 15 (until hatching; Figure 9), the skin of the flippers becomes thickened and the epidermis is composed of approximately 17 compact layers, and the dermis shows extensive supporting collagen fibers. Some digits in cross sections between the proximal and distal regions exhibit a cartilaginous core. Digits also begin the ossification process and develop the intricate Haversian systems; osteocytes are also visible at this Stage.

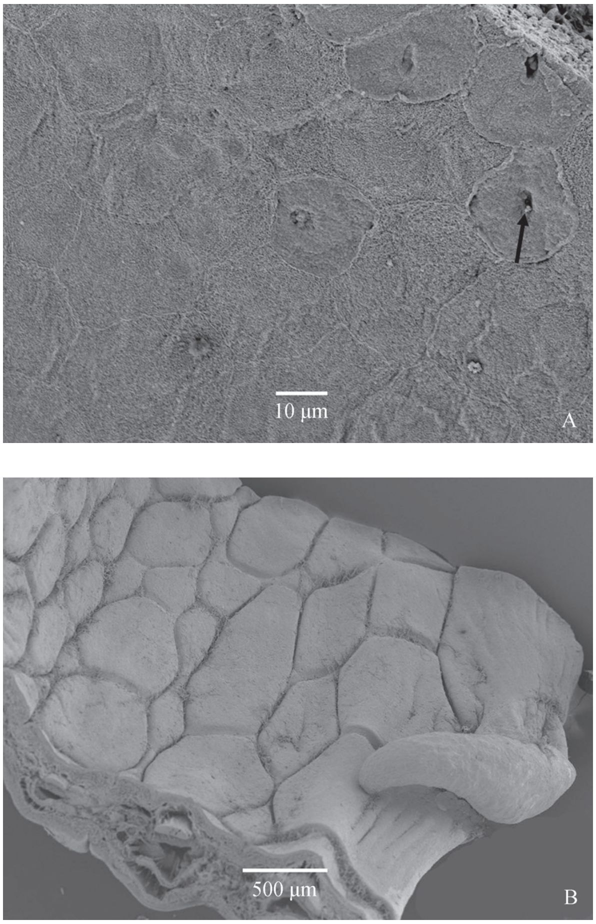

Figure 7 Electron micrographs of Stage 13 turtle embryo. A: Mucous pores in the epidermis (arrow); B: Scales and a claw on the ventral surface. Scale bar: A = 10 µm and B = 500 µm.

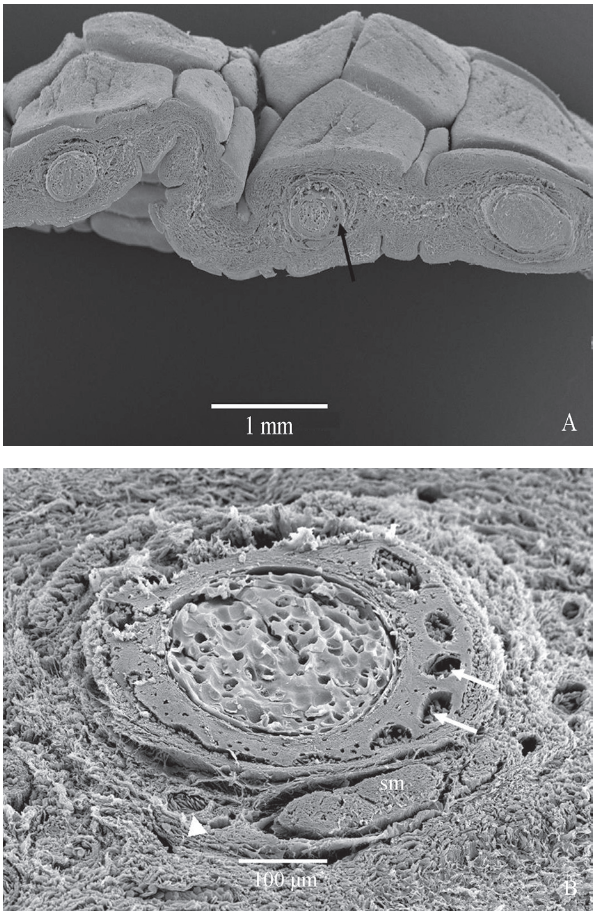

Figure 8 Electron micrographs of Stage 14 turtle embryo. A: Middle digit of the forelimb (arrows); B: Haversian system (arrows) and skeletal muscle bundles (sm). Scale bar: A = 1 mm and B = 100 µm.

Other digits show a spongy centre, which replaces the cartilaginous core in the middle of the digit. The initiation of endochondral ossification is associated with high vascularization. During the pipping stage, the outermost epidermal cells express well arranged boundaries with the presence of pores; some are associated with mucus secretions. Claws have become sharper and longer.

3.2 Transmission electron microscopy At Stage 5 (Figure 10), the epidermis has 2–3 layers of cells. The outer layer is composed of squamous cells with finger-like projections. The middle layer is composed of columnar cells exhibiting many spinous processes for the formation of intercellular junctions. The inner layer has a few germinative cells. The intercellular space is loose and filled with extracellular matrix. The dermis contains undifferentiated polygonal mesenchymal cells. These cells are sparsely distributed in the loose extracellular matrix with many processes. Cellular organelles, such as mitochondria, rough endoplasmic reticulum (RER), Golgi apparatus and ribosomes, are present.

At Stages 6 and 7 (Figure 11), the epidermis has 3–4 layers of cells. They form finger-like processes which form the future junctions. A number of cellular organelles such as mitochondria, lipid and mucus-granules are seen within these cells. The epidermal and dermal cells are joined by intercellular junctions. The amount of extracellular matrix becomes less at these stages as the cells become closer to each other. Gap junctions are common in the middle layer of the epidermis.

At Stage 8 (Figure 12), the large suprabasal cells of the middle layer of the epidermis have polygonal shapes and darker pigmentation, with many cytoplasmic extensions for the formation of intercellular junctions. Desmosomes and gap junctions appear clearly between those cells. Mitochondria in suprabasal cells are abundant in various shapes and sizes. The basement membrane shows dense attachment with collagenous fibers. Intercellular junctions such as gap junctions and desmosomes start to develop

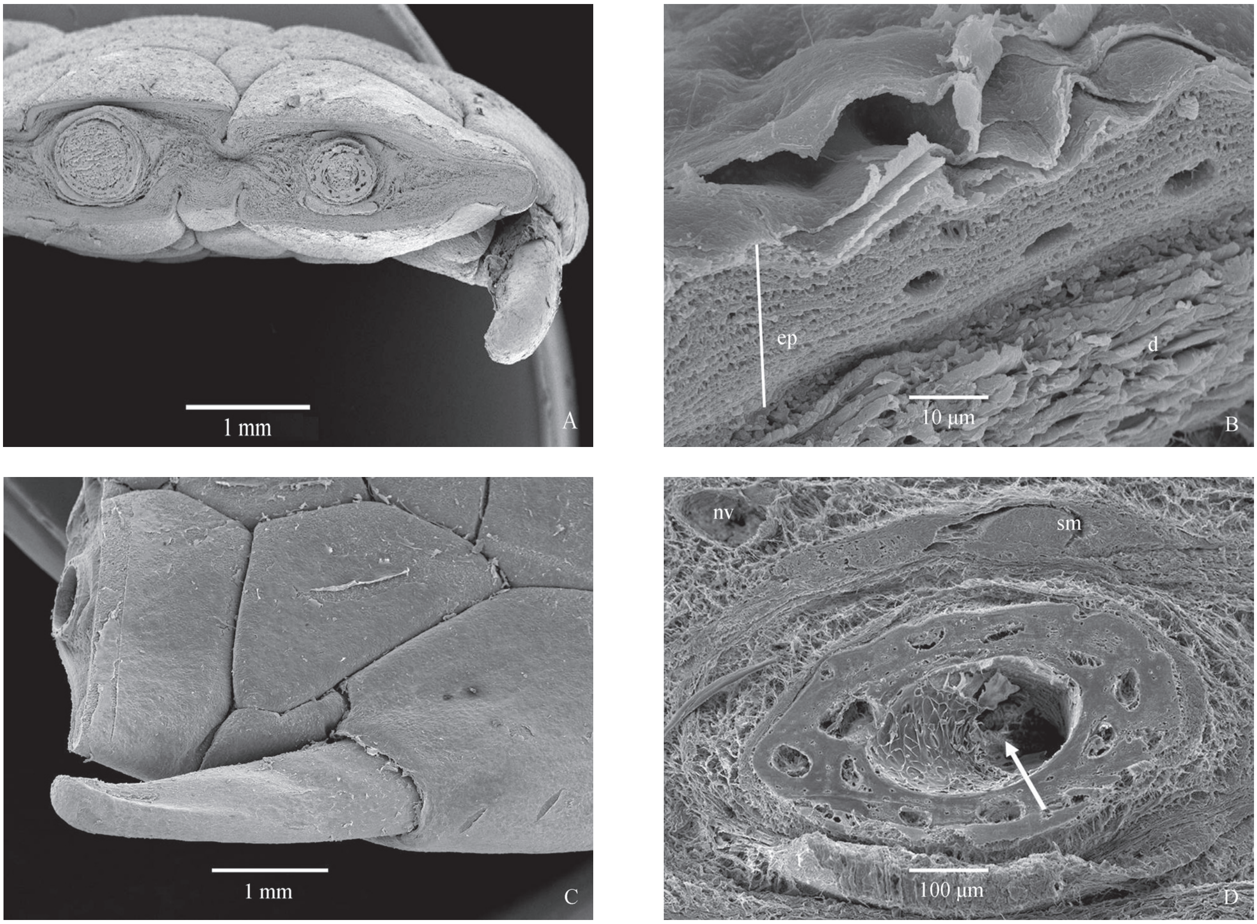

Figure 9 Electron micrographs of turtle embryos at Stage 15 (A and B), Stage 16 (C) and Stage 17 (D). A: Two digits, distal and middle digits; B: Epidermis (ep), dermis (d); C: the claw; D: A spongy core digit (white arrow), skeletal muscle bundles (sm) and nerve (nv). Scale bar: A = 1 mm, B = 10 µm, C = 1 mm and D = 100 µm.

between the dermal cells.

At Stages 9 and 10 (Figures 13 and 14), the epidermis has 6–7 layers of cells. Finger-like projections are seen on the outer surface of the epidermis. The basal cells become very stretched and wider than before, and express denser pigmentation and a higher number of intercellular junctions, hence, the spaces become narrower. The intercellular junctions take the appearance of comb-teeth. At Stage 11 (Figure 15), the intercellular matrix becomes denser than that at the previous stages. Many cells are found to have active mucus secretions with lipid vesicles.

4. Discussion

This study describes various morphological developmental changes during normal embryogenesis of the limb buds of the green turtle *C. mydas,* incubated in precision incubators at constant temperature. A precise incubation temperature is essential to eliminate temperature induced variation of the embryological feature within a developmental Stage. In this study, keeping the temperature consistent throughout the incubation period enabled us to compare the developmental events of the embryos at each stage without variation. This allowed us to describe each stage with accuracy relative to the consistent incubation temperature. The results obtained provide an overall understanding of the embryogenic events of limb development in this species.

Yntema (1978, 1979) and Miller (1982) considered the development of the limbs as the main feature for each embryonic stage. Limb length development is considered to be the most reliable feature of embryonic development (Miller, 1982). The forelimb length, ossification rate and skin pigmentation are considered to be the important features. However, these studies lacked description of tissue transformation at the ultrastructural level.

The AER is a transient embryonic structure essential for inducing proximo-distal patterning and outgrowth of the vertebrate limb (Lu *et al.,* 2008). It undergoes first a compaction process, whereby a distinctive narrow band of

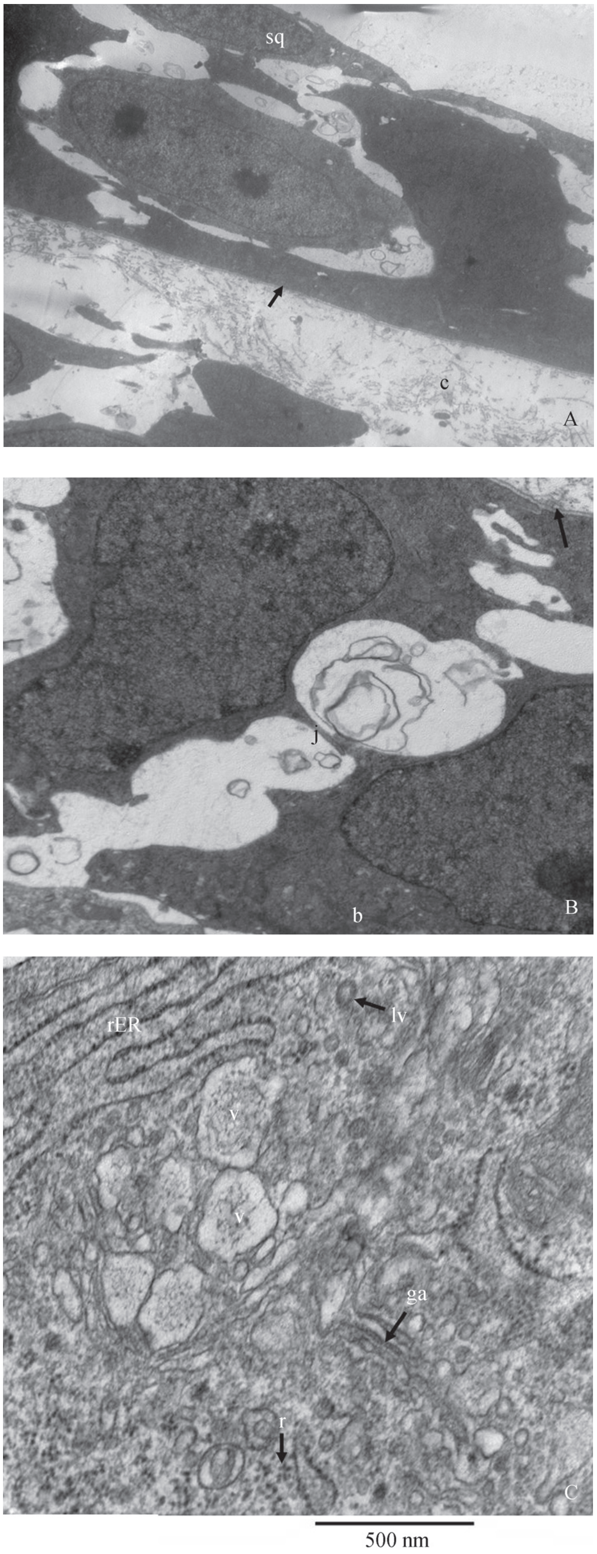

Figure 10 Electron micrographs of Stage 5 turtle embryo forelimb. A: Squamous cell of the epidermis (sq) with basal lamina (arrow), dermis with collagenous fibers (c) mitotic activities (mt); B: Intercellular junction (j), basal cells (b), microvilli on the surface of the epidermis (arrow heads); C: Rough endoplasmic reticulum (rER), lipid vesicles (lv), mucus-like vacuoles (v), Golgi apparatus (ga) and ribosomes (r). Scale bar: A = 2 μm, B and C = 500 nm.

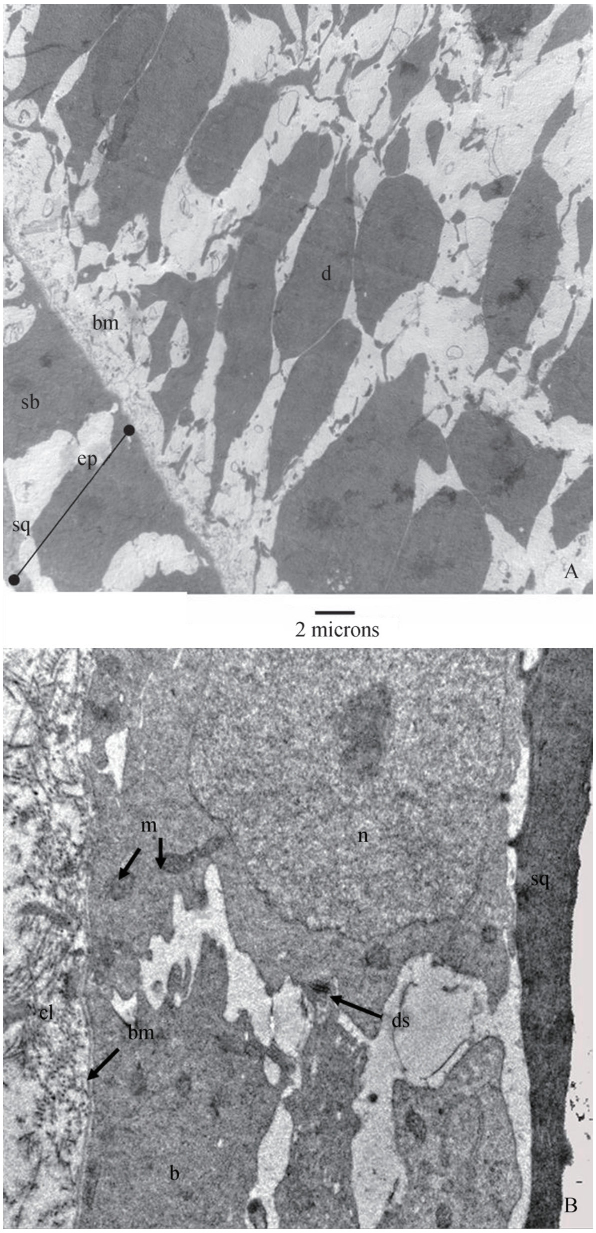

Figure 11 Electron micrographs of turtle embryos at Stage 6 (A) and Stage 7 (B). A: Epidermis layer (ep) with squamous cells (sq) and suprabasal cells (sb) lying on the basal lamina (bm) dermal cells (d); and B: desmosomal junctions (ds), basal cells(b), mitochondria (m), nucleus (n), basement membrane (bm) and collagenous fibers (cl). Scale bar: A = 2 μm and B = 1 μm.

stratified columnar epithelium forms at the early stages. The mature AER is then maintained between Stage 3 and Stage 5, while mesenchymal skeletal progenitors continue to proliferate and differentiate until a fully patterned limb is developed. The AER regresses via programmed cell death (Stage 6) and eventually flattens to a simple cuboidal epithelium. Lu *et al.* (2008) showed similar results in their study on mutant mice.

The forelimb and hindlimb of green turtles

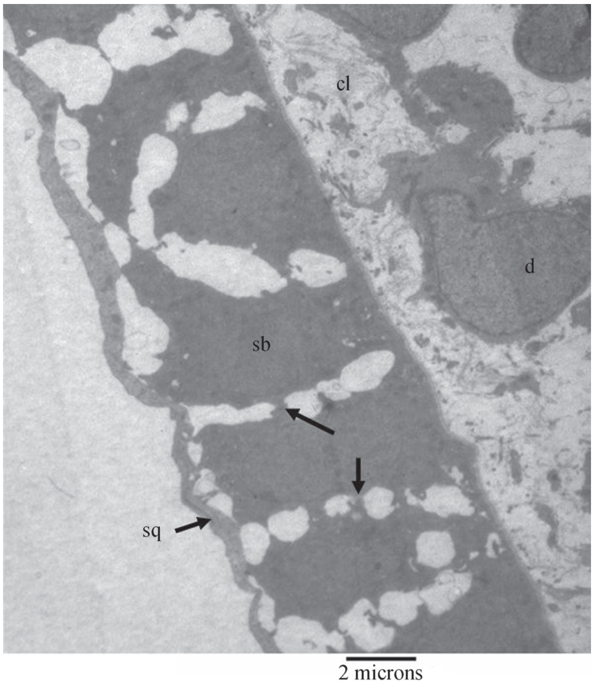

Figure 12 Electron micrograph of Stage 8 turtle embryo forelimb showing intercellular junctions (arrows) between the suprabasal cells (sb), squamous cells (sq) of the epidermis (ep), dermal cell (d), and collagen fibers (cl). Scale bar = 2 µm.

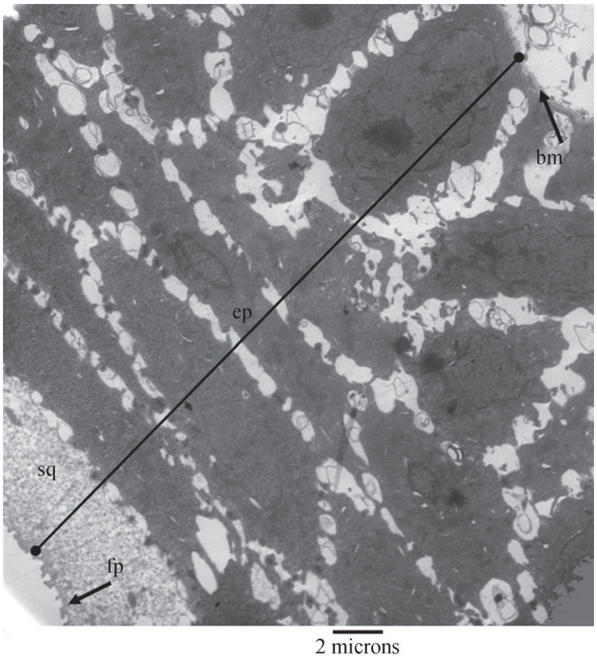

Figure 13 Electron micrographs of Stage 9 turtle embryo forelimb showing squamous cell (sq) with finger-like projections (fp), 6–7 cells layer of suprabasal cells, basal cell (bc) and basal lamina (bm). Scale bar = 2 µm.

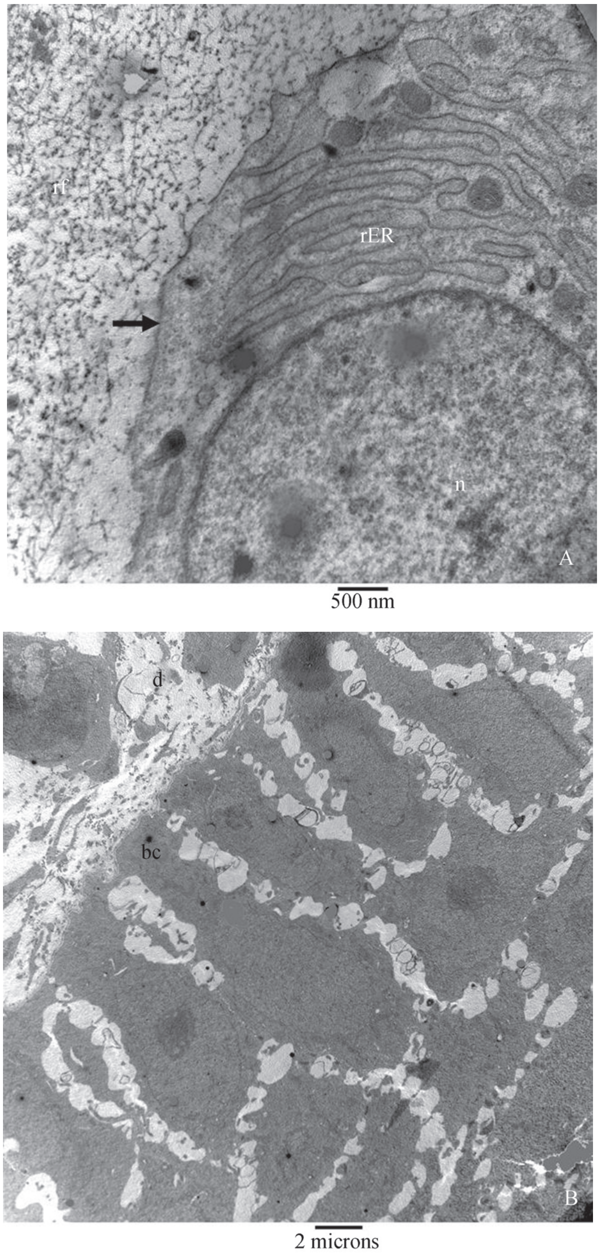

Figure 14 Electron micrographs of Stage 10 turtle embryo forelimb showing (A) rough endoplasmic reticulum (rER), reticular fibers (rf), nucleus (n) and cell membrane (arrow); and (B) epidermis with basal cell (bc) overlying the dermis (d). Scale bar: A = 500 nm and B = 2 µm.

develop almost in an identical fashion but with the hindlimb developmentally behind by approximately 12 h throughout the incubation period. This finding is in agreement with Miller's (1985) staging system. Richardson *et al.* (2009) reported a similar pattern of limb bud development in several chelonians and mammals.

In this study, the epidermis during the late stages of development showed stratification and thickening of the keratin. Microridges were also present in the outer epidermis. Alibardi (1999) also described the presence of microridges in the epidermis of the turtle *Emydura macquarii*. The extracellular dense deposits of mucus material were similar to those previously described by Matoltsy and Bednarz (1975). Mucus-secreting epidermis

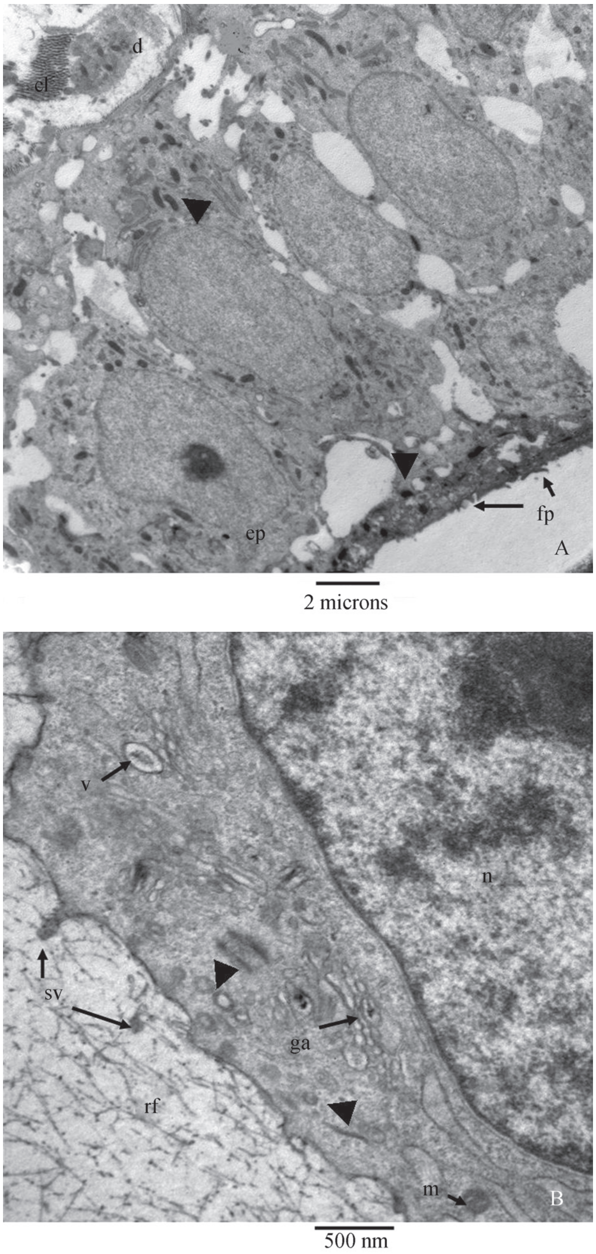

Figure 15 Electron micrographs of Stage 11 turtle embryo forelimb showing (A) squamous cells of the epidermis (ep), mitochondria (arrow head), finger-like projections (fp), dermis (d), collagen fibers (cl); and (B) intercellular matrix with reticular fibers (rf), lipid vesicles (arrow head), mucous-like vacuoles (v), Golgi apparatus (ga), secretory vesicles (sv) and nucleus (n). Scale bar: A = 2 μm and B = 500 nm.

was also described in birds (Mottet and Jensen, 1968) and in mammals (Bonneville, 1968).

At early stages, the predominant cells in the dermis are fibroblasts, which produce collagenous, elastic and reticular fibers, interacting with the epithelium, a pattern that was also described by Ross and Pawlina (2005).

Many cellular junctions were observed at different stages of limb development. The most frequent types are desmosomes and gap junctions and to a lesser extent tight junctions. Desmosomes frequently have been seen at earlier stages, which have been described in avian and mammalian epidermis (Mottet and Jensen, 1968). Desmosomes are associated with epidermal cohesiveness and cell stratification (Alibardi, 1999). Cell to cell communication through gap junctions allows the translocation of ions, metabolites and second messengers from cell to cell, which is essential for cellular functions such as cell growth, proliferation and differentiation (Ross and Pawlina, 2005).

Mesenchymal cells are divided into both chondrogenic and myogenic lineages that determine the differentiation of cartilage centrally and muscle peripherally (Sheil, 2005). This cellular differentiation was also observed at the early stages of the mesenchymal differentiation in the green turtle embryos. The condensation process of mesenchymal cells depends upon the signals initiated by cell-cell and cell-matrix interactions, and is associated with the increase in cell adhesion and formation of gap junctions and the changes in the cytoskeletal architecture (Goldring *et al.,* 2006). These ultrastructures are clear in our study.

This ultrastructural study may be the first study on limb bud formation in the green turtle, *C. mydas* with the hope that further research projects will be conducted in reference to molecular, genetics and hormonal regulations of limb buds in this species.

References

Alibardi L. 1999. Differentiation of the epidermis of neck, tail and limbs in the embryo of the turtle *Emydura macquarii.* Belgium J Zool, 129: 391–404

Al-Mukhaini N., Ba-Omar T., Mahmoud I., Al-Barwani S. 2010. Embryonic staging of the green turtles (*Chelonia mydas)*. Zool Middle East, 51: 39–50

Bonneville M. 1968. Observations on epidermal differentiation in the fetal rat. Am J Anat, 123: 147–164

Borkhvardt V. G. 2001. On the growth mechanics of the *Hynobiid* limb bud. Russ J Herpetol, 8(1): 54–58

Eichele G. 1990. Pattern formation in vertebrate limbs. Currt Opin Cell Biol, 2(6): 975–980

Goldring M. B., Tsuchimochi K., Ijiri K. 2006. The control of chondrogenesis. J Cell Biochem, 97: 33–44

Lu P., Yu Y., Perdue Y., Werb Z. 2008. The apical ectodermal ridge is a timer for generating distal limb progenitors. Development, 135: 1395–1405

Matoltsy A. G., Bednarz J. A. 1975. Lamellar bodies of the turtle epidermis. J Ultrastruct Res, 53: 128–132

Miller J. D. 1982. Development of Marine Turtles. Ph.D. Dissertation, Univ New England, Armidale, NSW, Australia

Miller J. D. 1985. Embryology of marine turtles. In Gans C., Billrtt

F., Maderson P. F. A. (Eds.), Biology of the Reptilia, Vol. 14 A. New York: Wiley-Interscience

Mottet N. K., Jensen H. M. 1968. The differentiation of chick embryonic skin. Exp Cell Res, 52: 261–283

Mrosovsky N. 1988. Pivotal temperatures for loggerhead turtles (*Caretta caretta*) from northern and southern nesting beaches. Can J Zool, 66: 661–669

Richardson M. K., Gobes S. M. H., Leeuwen A. C. V., Polman J. A. E., Pieau C., Sanchez-Villagra M. R. 2009. Heterochrony in limb evolution: Developmental mechanisms and natural selection. J Exp Zool, (Mol Dev Evol), 312B: 1–26

Ross M. H., Pawlina W. 2005. Histology a text and atlas with correlated cell and molecular biology (5th Ed). USA: Lippincott Williams & Wilkins

Salm R. V. 1991. Turtles in Oman: Status, threats and management options. IUCN Coastal Zone Management Project, 32 pp

Sakai H., Saeki K., Ichihashi H., Suganuma H., Shinsuke Tanabec S., Tatsukawad R. 2000. Species-specific distribution of heavy metals in tissues and organs of loggerhead turtle (*Caretta caretta*) and green turtle (*Chelonia mydas*) from Japanese coastal waters. Marine Pollut Bull, 40 (8): 701–709

Sánchez-Villagra M. R., Winkler J. D., Wurst L. 2007. Autopodial skeleton evolution in side-necked turtles (*Pleurodira*). Acta Zool (Stockholm), 88: 199–209

Sheil C. A. 2003. Osteology and skeletal development of *Apalone spinifera* (Reptilia: Testudines: Trionychidae). J Morphol, 256: 42–78

Sheil C. A. 2005. Skeletal development of *Macrochelys temminckii* (Reptilia: Testudines: Chelydridae). J Morphol, 263: 71–106

Sheil C. A., Greenbaum E. 2005. Reconsideration of skeletal development of *Chelydra serpentina* (Reptilia: Testudinata: Chelydridae): Evidence for intraspecific variation. J Zool, 265: 235–267

Yntema C. L. 1978. Incubation times for eggs of the turtle *Chelydra serpentine* (Testudines: Chelydridae) at various temperatures. Herpetologica, 34: 274–277

Yntema C. L. 1979. Temperature levels and periods of sex determination during incubation of eggs of *Chelydra serpentine*. J Morphol, 159: 17–28

Zeller R., Lopez-Rios, J., Zuniga A. 2009. Vertebrate limb bud development: moving towards integrative analysis of organogenesis. Nat Rev. (Genet), 10: 845–858